Selected Ion Flow Tube Studies of Air Plasma Cations Reacting with Alkylbenzenes

Susan T. Arnold,*,† Itzhak Dotan,‡ Skip Williams, A. A. Viggiano, and Robert A. Morris

Air Force Research Laboratory, Space Vehicles Directorate, 29 Randolph Road, Hanscom AFB, Massachusetts 01731-3010

Received: August 10, 1999; In Final Form: November 24, 1999

Rate constants and product branching fractions are reported for reactions of the air plasma cations NO^+, O_2^+, O^+, N^+, and N_2^+ with several alkylbenzenes: toluene, ethylbenzene, *n*-propylbenzene, and *m*-xylene. The measurements were made using a selected ion flow tube (SIFT) apparatus at 300 K. All reactions were found to proceed at the collision rate. NO^+ reactions yield exclusively nondissociative charge-transfer products. $C_7H_7^+$ is the dominant product ion observed in all the O^+, N^+, and N_2^+ reactions. Charge transfer and formation of $C_7H_7^+$ are the major product channels in the O_2^+ reactions. Product distributions were converted to crude breakdown diagrams, showing the relative abundance of each product ion as a function of the reactant ion recombination energy. The flow tube results exhibit a shift in the product ion threshold energies, an effect attributed to a kinetic shift resulting from slow fragmentation of the excited charge-transfer complex combined with collisional stabilization of the complex by the He buffer gas. Two isomeric forms of the $C_7H_7^+$ product ion are produced in these reactions: the benzyl (Bz^+) and tropylium (Tr^+) cations. The Bz^+/Tr^+ isomeric mixture ratio was quantified as a function of energy for all four alkylbenzenes. Changes in the Bz^+/Tr^+ mixture suggest that ethylbenzene has a relatively larger reverse activation barrier compared with toluene for forming Tr^+ from the charge-transfer complex, while formation of Tr^+ from the larger alkylbenzenes probably proceeds via a different mechanism altogether. For *m*-xylene, the formation of both Bz^+ and Tr^+ isomers likely proceeds via a different mechanism than for the *n*-alkylbenzenes.

Introduction

Gas-phase reactions between air positive ions and hydrocarbons have been studied over several decades both out of fundamental interest and for potential applications in several areas. Among the possible uses for kinetics information on these reactions are (1) schemes for chemical ionization detection of gas-phase hydrocarbons, (2) the potential enhancement of hydrocarbon combustion and ignition processes in the presence of ionization, (3) plasma processing schemes for the destruction of volatile organic compounds, and (4) application to the understanding and modeling of ionic molecular growth mechanisms.

Recent studies in our laboratory have focused on the notion of plasma-enhanced combustion of hydrocarbons. (Enhancing effects of ionization on hydrocarbon combustion have been noted in aeronautical engineering experiments but have not been explained.) Previously, we have examined the reactions of air plasma ions with a series of normal and branched alkanes for species up to dodecane and found a high degree of reactivity and numerous product channels involving alkane fragmentation.[1−3] Our preliminary modeling results,[4] in which ion−molecule kinetics were incorporated into a detailed neutral combustion kinetics model, have supported our speculation on the important role of ion−molecule reactions in the case of isooctane ignition. The modeling results indicate a decrease in ignition delay time with increasing levels of ionization, due largely to the early production of hydrocarbon free radicals.

We have recently completed a series of laboratory measurements examining the reactions of air plasma cations with several aromatic compounds, in part to extend the kinetics database to allow the continued modeling of fuel mixtures containing aromatic and aliphatic hydrocarbons. We have previously reported temperature-dependent rate constants and product distributions for reactions of air plasma cations with benzene and naphthalene.[5,6] In this paper we report 300 K rate constants and product branching fractions for reactions of NO^+, O_2^+, O^+, N^+, and N_2^+ with several alkylbenzenes: toluene, ethylbenzene, *n*-propylbenzene, and *m*-xylene (1,3-dimethylbenzene).

Experiment

The measurements were made using the Air Force Research Laboratory's variable temperature selected ion flow tube (SIFT). This instrument has been described previously in detail.[7] Reactant ions were produced by electron impact on a precursor compound, mass-selected in a quadrupole mass filter, and injected into the flow tube through a Venturi inlet into a fast flow of He buffer gas (∼100 m s^{-1}). The buffer gas (He, 99.997%) was passed through a molecular sieve/liquid nitrogen trap to reduce residual water vapor. The flow tube was maintained at a total pressure of ∼0.45 Torr. Neutral reactants were introduced downstream through a finger inlet, $^1/_8$ in. tubing that enters the flow tube perpendicular to the flow, terminating at the radial center of the flow tube. The hydrocarbon reactants were obtained commercially (99% Aldrich) and were used without further purification except for repeated freeze−pump−thaw cycles to eliminate dissolved gases. The toluene experiments utilized neat vapor as the reactant gas. Combinations of neat vapor and gas mixtures were used in the ethylbenzene and *m*-xylene experiments. Propylbenzene was introduced into the

* To whom correspondence should be addressed.
† Under contract to Aerodyne Research, Billerica, MA.
‡ NRC Senior Research Fellow. Permanent address: Department of Natural and Life Sciences, The Open University of Israel, 16 Klausner St. Ramat-Aviv, Tel-Aviv, Israel.

10.1021/jp9928199 CCC: $19.00 © 2000 American Chemical Society
Published on Web 01/14/2000

flow tube through a bubbler system where helium carrier gas was passed through a sample of propylbenzene. The flow rate of propylbenzene was derived from the known vapor pressure at a given temperature along with the helium flow rate and the total pressure in the bubbler; the propylbenzene flow rate was roughly proportional to the square root of the helium flow rate.[8] A small fraction of the gas in the tube flowed through a sampling orifice, and the reactant and product ions in this flow were mass-analyzed in a second quadrupole mass filter and detected by a particle multiplier. The reaction time was determined from previous time-of-flight measurements.

Rate constants were extracted from least-squares fits of the logarithm of the reactant ion signal versus the concentration of the neutral reactant. The accuracy of the measured overall rate constants is ±25%, and the relative accuracy is ±15%. Collisional rate constants were calculated using the parametrized trajectory model of Su and Chesnavich.[9,10]

Product branching fractions were determined by recording the product ion count rates as a function of the neutral reactant flow rate. To account for the effects of secondary reactions between the product ions and the neutral reactant, the reported branching percentages were determined by extrapolating the measured branching fractions to a neutral reactant flow rate of zero. Branching measurements were obtained by operating the mass spectrometer at two different resolution settings. A higher-resolution setting was used to determine the branching ratios between product ions of similar mass (those separated by one or two hydrogen atoms), and this ratio was applied to lower-resolution data taken to minimize mass discrimination wherein the species of similar mass appeared as a single broad peak. Comparing the reactant ion signal loss to the sum of the product ion signals yields a maximum absolute uncertainty in the branching fractions of 25%. The relative error between the branching fractions of any given product ion and the major product is 10%.

The formation of electronically excited NO^+ and O^+ reactant ions was monitored by introducing a small flow of N_2 into the flow tube prior to introducing any hydrocarbon reactants. Only the excited electronic states of NO^+ and O^+ undergo charge transfer with N_2,[11] so it was possible to monitor the formation of N_2^+ and then vary source conditions until <2% of the reactant ions were being formed as NO^+* and O^+*. Similarly, the formation of N^+* was monitored using D_2; the ground-state reaction yields exclusively ND^+, while the reaction of metastable N^+ yields exclusively D_2^+.[12] Vibrationally excited states of NO^+, O_2^+, and N_2^+ were quenched prior to reaction by introducing a small flow of N_2 into the tube upstream of the reaction zone.[13]

Results

Total rate constants and product branching fractions measured at 300 K for the reactions of NO^+, O_2^+, O^+, N^+, and N_2^+ with toluene are presented in Table 1. The reactions all proceed at or near the collision rate. The NO^+ and O_2^+ reactions yield only nondissociative charge-transfer products. For the reactant ions with larger recombination energies, the dominant product channel is $C_7H_7^+$. The N^+ and N_2^+ reactions both yield approximately 10% $C_3H_n^+$−$C_5H_n^+$ products that involve breaking the six-membered benzene ring structure. The only appreciable difference between these two reactions is the number of hydrogens associated with the $C_5H_n^+$ and $C_6H_n^+$ product ions. The reaction of N_2^+ yields $C_6H_5^+$ and $C_5H_6^+$, while the reaction of N^+ yields $C_6H_6^+$ and $C_5H_5^+$ products.

Rate constants and product distributions for the reactions of air plasma cations with ethylbenzene are presented in Table 2.

TABLE 1: 300 K Rate Constants and Product Branching Fractions for Reactions of NO^+, O_2^+, O^+, N^+, and N_2^+ with Toluene

	rate [k_c] 10^{-9} cm^3/s	product channels	branching fraction
NO^+	1.6 [1.8]	$C_7H_8^+ + NO$	1.0
O_2^+	1.7 [1.8]	$C_7H_8^+ + O_2$	1.0
O^+	2.2 [2.3]	$C_7H_8^+ + O$	0.05
		$C_7H_7^+ + (H + O)$	0.93
		$C_6H_6^+ + (CH_2 + O)$	0.02
N^+	2.2 [2.5]	$C_7H_7^+ + (H + N)$	0.82
		$C_6H_6^+ + (CH_2 + N)$	0.07
		$C_5H_5^+ + (C_2H_3 + N)$	0.05
		$C_4H_4^+ + (C_3H_4 + N)$	0.02
		$C_3H_3^+ + (C_4H_5 + N$	0.04
N_2^+	1.9 [1.9]	$C_7H_7^+ + H + N_2$	0.85
		$C_6H_5^+ + CH_3 + N_2$	0.05
		$C_5H_6^+ + C_2H_2 + N_2$	0.02
		$C_4H_4^+ + C_3H_4 + N_2$	0.05
		$C_3H_3^+ + C_4H_5 + N_2$	0.03

TABLE 2: 300 K Rate Constants and Product Branching Fractions for Reactions of NO^+, O_2^+, O^+, N^+, and N_2^+ with Ethylbenzene

	rate [k_c] 10^{-9} cm^3/s	product channels	branching fraction
NO^+	2.0 [2.0]	$C_8H_{10}^+ + NO$	1.0
O_2^+	2.2 [1.9]	$C_8H_{10}^+ + O_2$	0.30
		$C_7H_7^+ + CH_3 + O_2$	0.67
		$C_6H_6^+ + C_2H_4 + O_2$	0.03
O^+	2.4 [2.6]	$C_8H_{10}^+ + O$	0.04
		$C_8H_9^+ + (H + O)$	
		$C_7H_7^+ + (CH_3 + O)$	0.87
		$C_6H_6^+ + (C_2H_4 + O)$	0.09
N^+	2.6 [2.7]	$C_8H_{10}^+ + N$	0.05
		$C_8H_9^+ + (H + N)$	0.04
		$C_8H_8^+ + (H_2 + N)$	0.02
		$C_7H_7^+ + (CH_3 + N)$	0.70
		$C_6H_6^+ + (C_2H_4 + N)$	0.12
		$C_5H_5^+ + (C_3H_5 + N)$	0.03
		$C_4H_4^+ + (C_4H_6 + N)$	0.02
		$C_3H_3^+ + (C_5H_7 + N)$	0.02
N_2^+	1.9 [2.0]	$C_8H_{10}^+ + N_2$	0.04
		$C_8H_9^+ + H + N_2$	0.08
		$C_7H_7^+ + CH_3 + N_2$	0.79
		$C_6H_6^+ + C_2H_4 + N_2$	0.09

The reactions all proceed at or near the collision rate. Nondissociative charge transfer is the only product channel of the NO^+ reaction. Although charge transfer remains a significant channel in the O_2^+ reaction, it is a minor channel in the O^+, N^+, and N_2^+ reactions. The dominant product ion for all reactions except that with NO^+ is $C_7H_7^+$. In addition to the primary product channel, which corresponds to loss of CH_3 from ethylbenzene, small channels corresponding to loss of H, H_2, and C_2H_4 are also observed in the reactions with the higher-energy ions. Ring opening products, $C_3H_n^+$−$C_5H_n^+$, are only observed in the N^+ reaction, with a total branching fraction of 0.07.

Rate constants and product distributions for the propylbenzene reactions are presented in Table 3. The reactions all proceed at the collision rate. The NO^+ reaction yields only nondissociative charge-transfer products. The dominant product for the other reactant ions is $C_7H_7^+$. The O^+ and N_2^+ reactions produce $C_7H_7^+$ almost exclusively, with only a minor channel of $C_6H_6^+$, while the O_2^+ and N^+ reactions yield more numerous products. The N^+ reaction yields a minor channel of $C_5H_5^+$, making it the only reactant ion in this series to exhibit even a minor amount of ring opening with propylbenzene.

Rate constants and branching fractions for the *m*-xylene reactions are presented in Table 4. The reactions all proceed at

TABLE 3: 300 K Rate Constants and Product Branching Fraction for Reactions of NO^+, O_2^+, O^+, N^+, and N_2^+ with *n*-Propylbenzene

	rate [k_c] 10^{-9} cm3/s	product channels	branching fraction
NO^+	2.1 [2.1]	$C_9H_{12}^+ + NO$	1.0
O_2^+	1.9 [2.0]	$C_9H_{12}^+ + O_2$	0.18
		$C_8H_9^+ + CH_3 + O_2$	0.02
		$C_7H_7^+ + C_2H_5 + O_2$	0.75
		$C_6H_6^+ + C_3H_6 + O_2$	0.05
O^+	2.6 [2.7]	$C_7H_7^+ + (C_2H_5 + O)$	0.94
		$C_6H_6^+ + (C_3H_6 + O)$	0.06
N^+	2.7 [2.8]	$C_9H_{12}^+ + N$	0.06
		$C_8H_9^+ + (CH_3 + N)$	0.05
		$C_7H_7^+ + (C_2H_5 + N)$	0.76
		$C_6H_6^+ + (C_3H_6 + N)$	0.11
		$C_5H_5^+ + (C_4H_7 + N)$	0.02
N_2^+	2.1 [2.1]	$C_7H_7^+ + C_2H_5 + N_2$	0.98
		$C_6H_6^+ + C_3H_6 + N_2$	0.02

TABLE 4: 300 K Rate Constants and Product Branching Fraction for Reactions of NO^+, O_2^+, O^+, N^+, and N_2^+ with *m*-Xylene

	rate [k_c] 10^{-9} cm^3/s	product channels	branching fraction
NO^+	2.1 [1.9]	$C_8H_{10}^+ + NO$	1.0
O_2^+	1.7 [1.8]	$C_8H_{10}^+ + O_2$	0.78
		$C_7H_7^+ + CH_3 + O_2$	0.22
O^+	2.3 [2.4]	$C_8H_{10}^+ + O$	0.03
		$C_8H_9^+ + (H + O)$	0.14
		$C_7H_7^+ + (CH_3 + O)$	0.79
		$C_6H_6^+ + (C_2H_4 + O)$	0.04
N^+	2.5 [2.6]	$C_8H_{10}^+ + N$	0.17
		$C_8H_9^+ + (H + N)$	0.09
		$C_8H_8^+ + (H_2 + N)$	0.02
		$C_7H_7^+ + (CH_3 + N)$	0.58
		$C_6H_6^+ + (C_2H_4 + N)$	0.10
		$C_5H_5^+ + (C_3H_5 + N)$	0.02
		$C_4H_4^+ + (C_4H_6 + N)$	0.02
N_2^+	2.0 [1.9]	$C_8H_{10}^+ + N_2$	0.07
		$C_8H_9^+ + H + N_2$	0.36
		$C_7H_7^+ + CH_3 + N_2$	0.53
		$C_6H_6^+ + C_2H_4 + N_2$	0.04

or near the collision rate. The NO^+ reaction yields only nondissociative charge-transfer products. Charge transfer remains the dominant product channel for the O_2^+ reaction; however, a significant channel of $C_7H_7^+$ is also observed. For the O^+, N^+, and N_2^+ reactions, $C_7H_7^+$ is the dominant product ion. A significant channel corresponding to loss of H from *m*-xylene is also observed. N^+ is the only reactant ion that fragments the six-membered ring, with ring opening accounting for 4% of the total product ions.

The reactions of NO^+ and O_2^+ with toluene, ethylbenzene, propylbenzene, and *m*-xylene have previously been reported by Spanel and Smith.[14] The rate constants and product distributions reported here are generally in agreement with these earlier results with the exception of the O_2^+ reaction with propylbenzene. Spanel and Smith identify only two ionic products for this reaction, $C_7H_7^+$ and $C_6H_6^+$, with branching percentages of 80 and 20%, respectively. We observe the major $C_7H_7^+$ channel (75%), but we find that $C_6H_6^+$ is a minor channel (5%) and that additional products at $C_9H_{12}^+$ (18%) and $C_8H_9^+$ (2%) account for the remainder.

The major product ion of nearly all the alkylbenzene reactions, $C_7H_7^+$, exists in the gas phase as at least two discrete structures: the six-membered ring benzylium (Bz^+) and the seven-membered ring tropylium (Tr^+) isomers. The isomers can be distinguished from each another by their reactivity toward the parent compound. The Tr^+ isomer is unreactive toward toluene, while Bz^+ reacts with toluene via methylene transfer,[15−17]

$$C_7H_7^+ (Bz^+) + C_7H_8 \rightarrow C_8H_9^+ + C_6H_6 \quad (1)$$

In high-pressure mass spectrometric studies, an association channel was also observed for the reaction of toluene with the Bz^+ isomer.[18,19] Similarly, the Bz^+ isomer reacts with ethylbenzene (C_8H_{10}), propylbenzene (C_9H_{12}), and *m*-xylene (m−C_8H_{10}) via hydride transfer and/or methylene transfer:[15]

$$C_7H_7^+ (Bz^+) + C_8H_{10} \rightarrow C_8H_9^+ + C_7H_8$$
$$\rightarrow C_9H_{11}^+ + C_6H_6 \quad (2)$$

$$C_7H_7^+ (Bz^+) + C_9H_{12} \rightarrow C_9H_{11}^+ + C_7H_8$$
$$\rightarrow C_{10}H_{13}^+ + C_6H_6 \quad (3)$$

$$C_7H_7^+ (Bz^+) + m\text{-}C_8H_{10} \rightarrow C_9H_{11}^+ + C_6H_6 \quad (4)$$

As with toluene, association products were also observed for the reactions of ethylbenzene, propylbenzene, and *m*-xylene with the Bz^+ isomer. The Tr^+ isomer is presumed to be unreactive toward ethylbenzene, propylbenzene, and *m*-xylene as it is with toluene.[15]

The Tr^+/Bz^+ isomeric mixture was determined by following the $C_7H_7^+$ secondary ion chemistry to completion and equating the unreactive component to the Tr^+ isomer. For each alkylbenzene, the isomeric mixture was measured for two ion reactions, the reaction that first yields $C_7H_7^+$ product ions (either O_2^+ or O^+) and the highest-energy reactant ion N_2^+. The results are shown in Table 5. For all these compounds, there is virtually no change in the isomeric mixture with increasing reaction energy, even for the *m*-xylene reactions where there is a significant change in the overall product distribution over the same energy range. For toluene, ethylbenzene, propylbenzene, and *m*-xylene, the average fraction of $C_7H_7^+$ products formed with the Bz^+ structure is 0.56, 0.68, 0.92, and 0.75, respectively.

TABLE 5: Bz^+ and Tr^+ Isomeric Mixture of $C_7H_7^+$ Product Ions

	fraction of $C_7H_7^+$ product formed as Bz^+ in ion−molecule reaction			
reactant	O_2^+	O^+	N_2^+	av Bz^+/Tr^+
toluene		0.59	0.53	1.3
ethylbenzene	0.66		0.68	2.0
propylbenzene	0.91		0.93	12
m-xylene	0.78		0.72	3.0

Discussion

Breakdown Curves. The relative abundance of the parent ion and various product ions as a function of energy constitutes the breakdown diagram of a particular species. We have previously shown that product distributions from charge-transfer reactions measured in flow tube experiments can be used to construct breakdown diagrams for benzene[5] and naphthalene.[6] Praxmarer et al.[20] have also constructed breakdown diagrams for several small hydrocarbons using the product distributions from charge-transfer reactions measured in a flow tube.

By use of the product distributions shown in Tables 1−4, crude breakdown diagrams for toluene, ethylbenzene, propylbenzene, and *m*-xylene were constructed, and these are shown in Figure 1. The relative abundances of the parent and product ions are shown as a function of the reactant ion recombination energy (NO^+ = 9.26 eV, O_2^+ = 12.07, O^+ = 13.62 eV, N_2^+ =

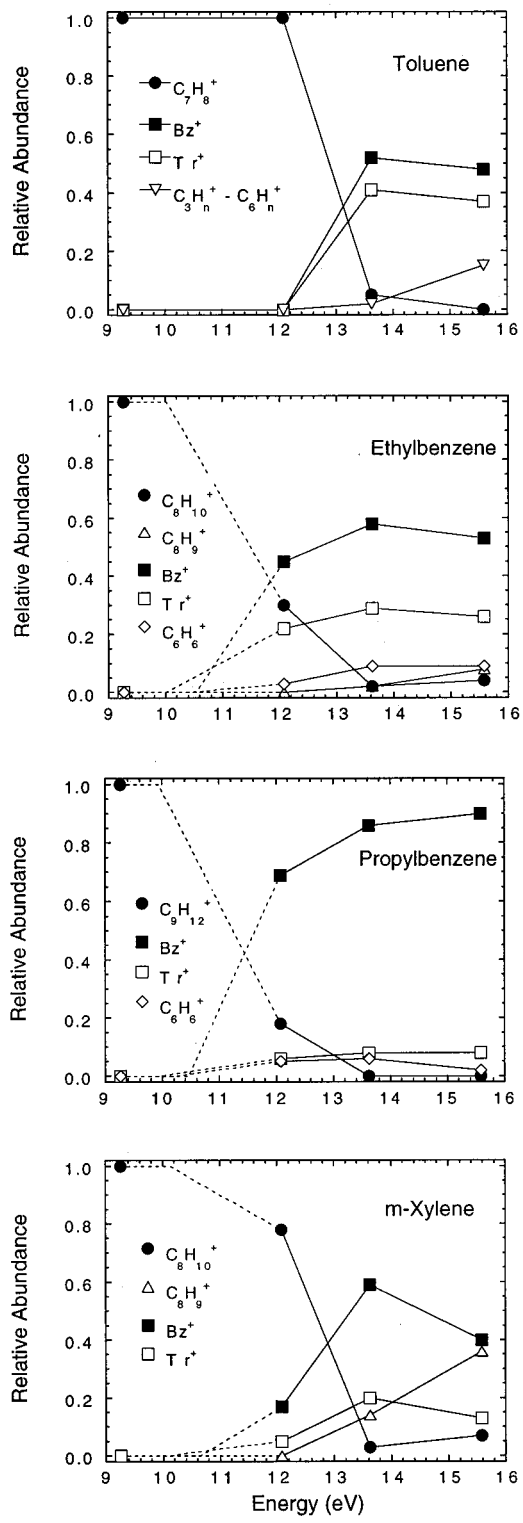

Figure 1. Product distributions for the charge-transfer reactions of NO^+, O_2^+, O^+, and N_2^+ with toluene, ethylbenzene, propylbenzene, and *m*-xylene converted to rough breakdown diagrams. The energy scale does not include the internal energy of the reactants and represents only the recombination energy of the reactant ions: $NO^+ = 9.26$ eV, $O_2^+ = 12.07$ eV, $O^+ = 13.62$ eV, and $N_2^+ = 15.58$ eV. Dashed lines are shown to indicate where individual product channels become energetically accessible. All thresholds were calculated assuming no barriers to formation.

15.58 eV). The internal energy of the reactants, which is approximately 0.2−0.3 eV at 300 K, has not been included in the energy scale. The lines are an interpolation through the NO^+, O_2^+, O^+, and N_2^+ data and are only meant to guide the eye. The N^+ data (recombination energy of 14.53 eV) have not been included for reasons that are explained below. Because the entire metastable decay regions for ethylbenzene, *m*-xylene, and propylbenzene were not probed directly, dashed lines are shown to indicate where individual product channels become energetically accessible. All thresholds, except for formation of Tr^+ from toluene, were calculated assuming no barrier to formation. Separate curves are shown for the two isomers of $C_7H_7^+$, where the average Bz^+/Tr^+ ratios from Table 5 have been applied to the individual product distributions in order to obtain different curves for each isomer.

In the toluene charge-transfer reactions, the parent ion decays above 12 eV, forming nearly equal amounts of Bz^+ and Tr^+ $C_7H_7^+$ isomers. Only very small amounts of other product ions are observed. It has been shown previously that the appearance energies to form Tr^+ and Bz^+ from toluene are very similar, 10.94 and 11.01 eV, respectively.[21] However, in the flow tube study, we do not observe any $C_7H_7^+$ products with O_2^+ reactant ions, which have a recombination energy of over 12 eV. Spanel and Smith[14] also report only nondissociative charge-transfer products in their flow tube study of the O_2^+ reaction with toluene. There is an apparent shift in the flow tube dissociation threshold energy of at least 1 eV. Similar differences in flow tube dissociation thresholds were observed for benzene and naphthalene.[5,6] For benzene, the difference in threshold energies was attributed to the energized charge-transfer complex being collisionally stabilized by interactions with the He buffer, therefore requiring higher internal energies for dissociation. The threshold energy shift for naphthalene was much larger and was attributed to a collisional stabilization effect and to a significant kinetic shift that results from slow dissociation of the energized charge-transfer complex. Huang and Dunbar[22] have reported energy-dependent dissociation rates for the toluene cation, which allows the kinetic shift to be estimated. We anticipate a kinetic shift of approximately 0.6 eV in the flow tube experiments due to the slow dissociation rate of the toluene cation. Because the kinetic shift only partially explains the difference in threshold energies, we attribute the remainder to collisional stabilization of the energized charge-transfer complex by the He buffer, similar to what we have previously observed for benzene and naphthalene charge-transfer reactions in the flow tube.[5,6]

Although we do not probe the entire metastable decay region for the larger alkylbenzenes, it seems likely that dissociation thresholds are affected by kinetic shifts and collisional stabilization as well. Beyond the metastable decay region, the breakdown curves are unaffected by these factors because the dissociation rates are rapid. For ethylbenzene and propylbenzene, $C_7H_7^+$ is the dominant product ion, and only small amounts of other products are observed. The Tr^+ branching fraction decreases from toluene to ethylbenzene to propylbenzene, while the Bz^+ branching fraction increases, especially between ethylbenzene and propylbenzene. For *m*-xylene, $C_7H_7^+$ is the major product ion at threshold and at energies slightly above the metastable decay region; however, by 16 eV, $C_8H_9^+$ is becoming the major product ion.

The breakdown diagram of the *n*-butylbenzene cation has been reported previously by Baer et al.[23] Dissociation results in formation of both $C_7H_7^+$ and $C_7H_8^+$ product ions, and the branching ratio changes dramatically with the internal energy of the parent ion. Baer et al. conclude that (1) the threshold for formation of $C_7H_7^+$ lies 0.6 eV above the $C_7H_8^+$ onset and that (2) both energetic and mechanistic considerations are consistent with the production of only the Bz^+ isomer of $C_7H_7^+$. The lack

of Tr^+ products from *n*-butylbenzene is not surprising given the trend observed from toluene, ethylbenzene, and *n*-propylbenzene.

Although formation of $C_7H_8^+$ from ethylbenzene is an energetically accessible product channel for O^+, N^+, and N_2^+ reactant ions, and it is an accessible channel from propylbenzene for all reactant ions except NO^+, no $C_7H_8^+$ products were observed in reactions with ethylbenzene or propylbenzene. Spanel and Smith[14] also report no $C_7H_8^+$ products being formed in the reaction of O_2^+ with propylbenzene.

The results of the N^+ reactions are not included in Figure 1 because it seems likely that these reactions do not involve exclusively charge-transfer processes. In our previous study of charge-transfer reactions with benzene, the product distribution from the N^+ reaction was anomalous in many ways. Although similar reaction product ions were observed in the N^+ reaction with benzene as in other charge-transfer reactions (mass assignments confirmed using $^{15}N^+$ reactants), several products appeared to form below threshold. In addition, we were not able to model the pressure dependence of the N^+ product distrubutions using a dissociative charge-transfer model. For these reasons, we concluded that the N^+ reaction involves both reactive and charge-transfer channels and that in at least one case, the reactive channel involves incorporation of the N atom into the neutral products.[5] The product distributions from the N^+ reactions with alkylbenzenes are also anomalous compared to the other air plasma cation reactants. In general, the N^+ reactions always yield more nondissociative charge transfer and $C_6H_6^+$ products and less $C_7H_7^+$ products compared to what is expected from the breakdown diagrams in Figure 1. In addition, N^+ is the only reactant that results in loss of H_2 from ethylbenzene and *m*-xylene, and it is the only reactant that yields $C_5H_n^+$ or smaller product ions from ethylbenzene, *m*-xylene, and propylbenzene. In Tables 1−4, the neutral products of the O^+ and N^+ dissociative charge-transfer reactions are shown in parentheses, indicating that their assignment is uncertain. Although all the reaction channels are exothermic as written, reactions that incorporate the O or N radical into the neutral product are significantly more exothermic. The fact that slightly different $C_5H_n^+$ and $C_6H_n^+$ product ions are observed in the N^+ and N_2^+ reactions with toluene may indicate that this reaction involves C−N bond formation in the neutral products as is suspected in the benzene reaction.

$$N_2^+ + C_7H_8 \rightarrow C_6H_5^+ + CH_3 + N_2 \quad (5a)$$

$$\rightarrow C_5H_6^+ + C_2H_2 + N_2 \quad (5b)$$

$$N^+ + C_7H_8 \rightarrow C_6H_6^+ + (H + HCN) \quad (6a)$$

$$\rightarrow C_5H_5^+ + (CH_2 + HCN) \quad (6b)$$

Bz^+ and Tr^+ Isomers. The formation of $C_7H_7^+$ product ions from toluene has been studied extensively, and a comprehensive review is provided by Lifshitz.[21] The schematic potential energy diagram showing the formation of Bz^+ and Tr^+ isomers of $C_7H_7^+$ from $C_7H_8^+$ has been calculated by Lifshitz et al.[24] and is shown in Figure 2 as a solid line. Two discrete isomers are formed in a complex isomerization/dissociation reaction. Although the Tr^+ isomer is 46 kJ mol^{-1} more stable than the Bz^+ isomer, these species have nearly identical appearance energies because there is a 42 kJ mol^{-1} reverse activation barrier associated with forming Tr^+ from $C_7H_8^+$. The $Bz^+ \Leftrightarrow Tr^+$ isomerization has been examined by Smith and Hall,[25] and the results of their calculation are also reproduced in Figure 2 as a dashed line. Isomerization of Bz^+ to Tr^+ proceeds through a single intermediate and requires an activation energy of 272 kJ mol^{-1}. In the flow tube measurements with toluene, the ratio of $C_7H_7^+$ isomers was measured in an energy range that corresponds to 250−435 kJ mol^{-1} above the $C_7H_7^+$ formation threshold. Therefore, isomerization between the two $C_7H_7^+$ isomers is a possibility through most but not all of the energy range we examined. As shown in Table 5, a relatively constant Bz^+/Tr^+ ratio was observed, suggesting that isomerization of $C_7H_7^+$ (as opposed to isomerization of $C_7H_8^+$) does not play an important role. The fact that nearly equal amounts of Bz^+ and Tr^+ isomers are formed from these charge-transfer reactions is consistent with the surface as shown in Figure 2, where nearly equal activation energies are required to form either isomer. Previous examinations of the $C_7H_7^+$ isomeric ion mixture in charge exchange experiments[26] report 60−65% Bz^+ in this energy range, while collisional activation mass spectra[27] demonstrate that at the lowest energies attainable, the fraction of $C_7H_7^+$ ions formed with the Bz^+ structure was 50%. These values are in agreement with the present values of 53−59%.

In the ethylbenzene flow tube studies, the isomeric mixture was measured over an energy range that corresponds to 150−490 kJ mol^{-1} above the Bz^+ formation threshold. Throughout this range, a constant Bz^+/Tr^+ ratio was observed, suggesting that isomerization between Bz^+ and Tr^+ is not an important factor. The overall branching fraction of Bz^+ is similar in the toluene and ethylbenzene charge-transfer reactions. However, there is a significant decrease in the overall Tr^+ branching fraction for the ethylbenzene reaction; thus, the Bz^+/Tr^+ ratio is higher in the ethylbenzene reaction.

Qualitatively, one might expect the ethylbenzene cation to have a reaction potential energy surface similar to that shown for toluene in Figure 2, forming Bz^+ by direct cleavage of a methyl group (in comparison to H cleavage) and Tr^+ via a six- to seven-membered-ring isomerization followed by cleavage of the alkyl group. The Bz^+ and Tr^+ dissociation limits are lower in energy for ethylbenzene because the C−C bond energy is lower than the C−H bond energy. Since there is no activation energy besides the endothermicity in forming Bz^+, the energy required to form this isomer is lower for the ethylbenzene reaction. The height of any barriers along the path to form Tr^+ is uncertain. The late barrier again reflects the difference in breaking a C−C bond vs a C−H bond in the two systems and is likely to be smaller in the ethylbenzene case. The early barrier involves a similar hydrogen migration in the two systems and should be comparable in the two systems. With these assumptions, the increasing Bz^+/Tr^+ ratio reflects the lowering of the formation energy for Bz^+ only.

Previous low-pressure charge exchange experiments[26] determined that approximately 85% of $C_7H_7^+$ ions formed from ethylbenzene in this energy range have the Bz^+ structure. This is significantly larger than the 67% reported here. As pointed out above, we expect pressure effects are influencing the branching ratios, and the discrepancy between the two experiments may be a pressure dependence.

For the propylbenzene flow tube studies, the isomeric mixture was measured over an energy region corresponding to 155−492 kJ mol^{-1} above the Bz^+ formation threshold. As with the other *n*-alkylbenzenes, a constant Bz^+/Tr^+ ratio was observed over this energy range, suggesting that isomerization between the $C_7H_7^+$ isomers is not an important factor. Compared to ethylbenzene and toluene, there is a continued decrease in the Tr^+ branching fraction and a significant increase in the overall

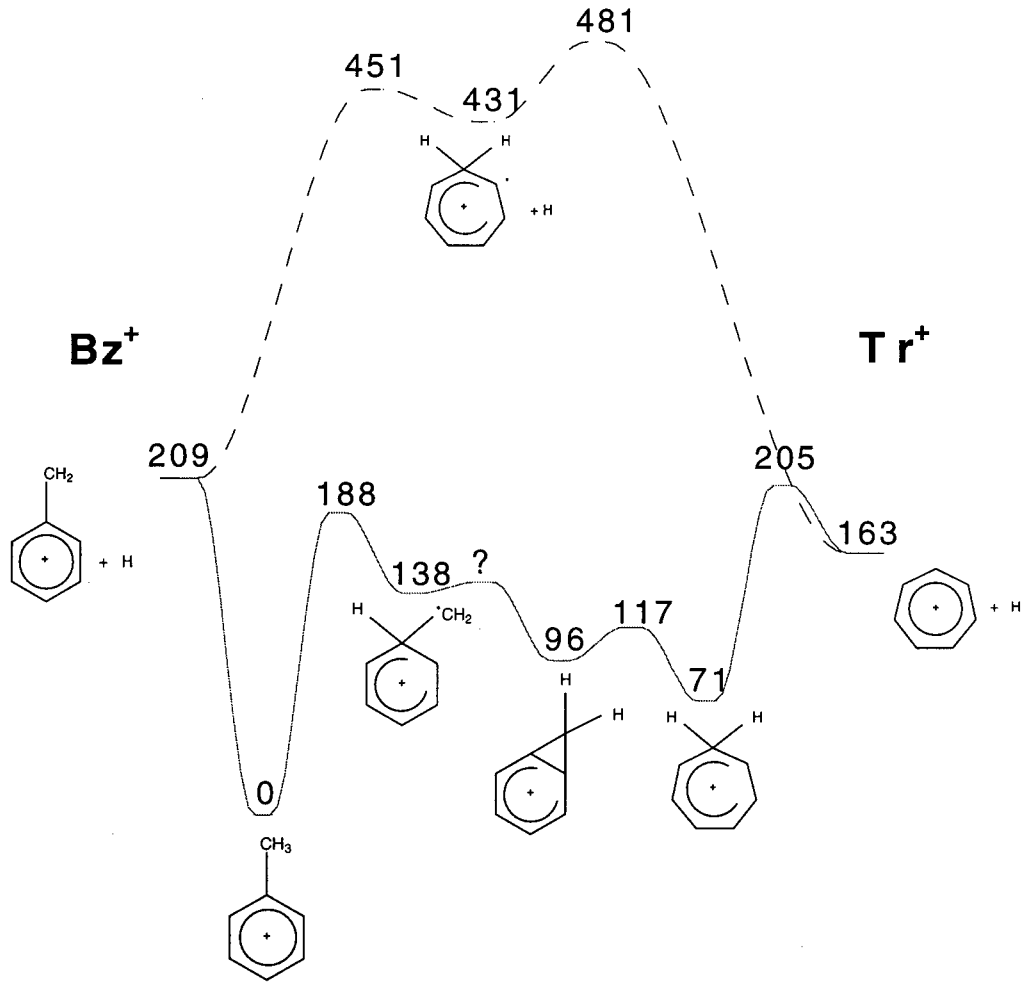

Figure 2. Schematic potential energy diagram showing the formation of Bz^+ and Tr^+ isomers of $C_7H_7^+$ from $C_7H_8^+$ as calculated by Lifshitz et al.[24] is shown as a solid line. The isomerization of Bz^+ to Tr^+, as calculated by Smith and Hall,[25] is also shown as a dashed line. The standard energy of a hydrogen atom is added to put the two curves on the same scale. All energies are in kJ mol^{-1}.

Bz^+ branching fraction. Above the metastable decay region, the Bz^+ isomer has branching fractions approaching 90%, and the Tr^+ branching fractions are less than 8%.

Qualitatively, these results are not consistent with the $C_7H_7^+$ reaction surface described above for toluene and ethylbenzene. For propylbenzene, the Tr^+ and Bz^+ dissociation limits are nearly equal to the corresponding ethylbenzene Tr^+ and Bz^+ product channels. In addition, one might expect the barriers associated with the initial hydrogen migration and the final alkyl cleavage for ethylbenzene and propylbenzene to be rather similar. Overall, this would suggest a Bz^+/Tr^+ profile for propylbenzene that is very similar to that of ethylbenzene. However, a significant difference is observed between these two compounds. Because Bz^+ is most likely formed via a direct bond cleavage, the flow tube results suggest that the mechanism to form Tr^+ is qualitatively different from the scheme outlined in Figure 2 for toluene. Perhaps the longer alkyl side chain plays a significant role (i.e., through ring formation), interfering with the initial hydrogen migration or final alkyl cleavage steps. Note that for *n*-butylbenzene, Baer et al.[23] suggest that the $C_7H_7^+$ product ion formed is exclusively the Bz^+ isomer. This is consistent with our speculation that propylbenzene and larger *n*-alkylbenzenes have a different $C_7H_7^+$ dissociation mechanism than toluene and ethylbenzene.

The formation of $C_7H_7^+$ product ions from *m*-xylene dissociation is distinctly different from $C_7H_7^+$ formation from the other alkylbenzenes included in this study. Unlike the *n*-alkylbenzenes, the Bz^+ isomer of $C_7H_7^+$ cannot be formed from *m*-xylene by direct cleavage of an alkyl group with no subsequent hydrogen migration. Presumably, the reaction paths for both Bz^+ and Tr^+ formation begin by cleavage of a methyl group from $C_8H_{10}^+$ to give $C_7H_7^+$ followed by rearrangement(s) to yield either Tr^+ or Bz^+. We do not know the threshold for Bz^+ or Tr^+ formation because both pathways likely involve barriers, and there are no reliable appearance energy determinations. Over the energy range we examined, we observed a relatively constant Bz^+/Tr^+ ratio, suggesting that there is still no isomerization between $C_7H_7^+$ isomers. The overall branching fraction of $C_7H_7^+$ changes significantly over this range, increasing dramatically in the metastable decay region and then decreasing as $C_8H_9^+$ products are formed in greater abundance.

Summary

The reactions of NO^+, O_2^+, O^+, N^+, and N_2^+ with several alkylbenzenes (toluene, ethylbenzene, *n*-propylbenzene, and *m*-xylene) all proceed at the collision rate. NO^+ reactions yield exclusively nondissociative charge-transfer products. $C_7H_7^+$ is the dominant product ion observed in all the O^+, N^+, and N_2^+ reactions. Charge transfer and formation of $C_7H_7^+$ are the major product channels in the O_2^+ reactions. Rough breakdown diagrams for each compound reveal that (1) there is more fragmentation observed with the higher-energy ions (however, there is preferential cleavage of the alkyl side chain as opposed to cleavage of the aromatic ring) and that (2) several exothermic

reaction channels are not observed at their thermochemical threshold. The threshold energy difference was attributed to a kinetic shift, resulting from slow fragmentation of the energized charge-transfer complex, combined with collisional stabilization of the complex by the He buffer.

Two isomeric forms of the $C_7H_7^+$ product ion are produced in these reactions, the benzyl cation (Bz^+), a six-membered ring isomer, and the tropylium cation (Tr^+), a seven-membered ring isomer. The isomers were distinguished by their reactivity toward the parent aromatic compound. The percentage of $C_7H_7^+$ formed as the Bz^+ isomer remains fairly constant for each alkylbenzene over the energy range of these experiments, indicating that isomerization of Bz^+ to Tr^+ and vice versa are not an important factor. The change in the overall Tr^+ and Bz^+ branching fractions for toluene, ethylbenzene, propylbenzene, and *n*-butylbenzene suggest that ethylbenzene has a relatively larger reverse activation barrier compared to toluene for forming Tr^+ from the charge-transfer complex, while formation of Tr^+ from the larger alkylbenzenes probably proceeds via a different mechanism altogether. For *m*-xylene, the formation of both Bz^+ and Tr^+ isomers likely proceeds via a different mechanism than for the *n*-alkylbenzenes.

The reactions of N^+ with this series of alkylbenzenes demonstrate more complexity than reactions of other air plasma cations included in this study and may involve many noncharge-transfer processes.

Acknowledgment. Technical support from John Williamson and Paul Mundis is gratefully acknowledged. S.T.A. acknowledges Anthony Midey for his assistance in producing figures. This research was supported by the Air Force Office of Scientific Research under Project No. 2303EP4.

References and Notes

(1) Arnold, S. T.; Viggiano, A. A.; Morris, R. A. *J. Phys. Chem. A* **1997**, *101*, 9351.

(2) Arnold, S. T.; Viggiano, A. A.; Morris, R. A. *J. Phys. Chem. A* **1998**, *102*, 8881.

(3) Arnold, S. T.; Morris, R. A.; Viggiano, A. A. *J. Phys. Chem. A* **1998**, *102*, 1345.

(4) Williams, S.; Arnold, S. T.; Morris, R. A.; Maurice, L. Q.; Viggiano, A. A.; Bench, P.; Dotan, I.; Midey, A. J.; Morris, T.; Sutton, E. A. Proceedings of the 14th International Symposium on Air Breathing Engines, Florence, Italy, September 1999; ISABE-7236.

(5) Arnold, S. T.; Williams, S.; Dotan, I.; Midey, A. J.; Morris, R. A.; Viggiano, A. A. *J. Phys. Chem. A* **1999**, *103*, 8421.

(6) Midey, A. J.; Williams, S.; Arnold, S. T.; Dotan, I.; Morris, R. A.; Viggiano, A. A. *Int. J. Mass Spectrom.*, in press.

(7) Viggiano, A. A.; Morris, R. A.; Dale, F.; Paulson, J. F.; Giles, K.; Smith, D.; Su, T. *J. Chem. Phys.* **1990**, *93*, 1149.

(8) Viggiano, A. A.; Perry, R. A.; Albritton, D. L.; Ferguson, E. E.; Fehsenfeld, F. C. *J. Geophys. Res.* **1980**, *85*, 4551.

(9) Su, T.; Chesnavich, W. J. *J. Chem. Phys.* **1982**, *76*, 5183.

(10) Su, T. *J. Chem. Phys.* **1988**, *89*, 5355.

(11) Ikezoe, Y.; Matsuoka, S.; Takebe, M.; Viggiano, A. A. *Gas Phase Ion−Molecule Reaction Rate Constants Through 1986*; Maruzen Company, Ltd.: Tokyo, 1987.

(12) Tichy, M.; Rakshit, A. B.; Lister, D. G.; Twiddy, N. D.; Adams, N. G.; Smith, D. *Int J. Mass Spectrom. Ion Phys.* **1979**, *29*, 231.

(13) Ferguson, E. E. *J. Phys. Chem.* **1986**, *90*, 731.

(14) Spanel, P.; Smith, D. *Int. J. Mass Spectrom.* **1998**, *181*, 1.

(15) Jackson, J. A.; Lias, S. G.; Ausloos, P. *J. Am. Chem. Soc.* **1977**, *99*, 7515.

(16) Dunbar, R. C. *J. Am. Chem. Soc.* **1975**, *97*, 1382.

(17) Shen, J.; Dunbar, R. C.; Olah, G. A. *J. Am. Chem. Soc.* **1974**, *96*, 6227.

(18) Giardini-Guidoni, A.; Zocchi, Z. *Trans. Faraday Soc.* **1968**, *64*, 2342.

(19) Wexler, S.; Clow, R. P. *J. Am. Chem. Soc.* **1968**, *90*, 3940.

(20) Praxmarer, C.; Hansel, A.; Lindinger, W.; Herman, Z. *J. Chem. Phys.* **1998**, *109*, 4246.

(21) Lifshitz, C. *Acc. Chem. Res.* **1994**, *27*, 138.

(22) Huang, F.-S.; Dunbar, R. D. *J. Am. Chem. Soc.* **1990**, *112*, 8167.

(23) Baer, T.; Dutuit, O.; Mestdagh, H.; Rolando, C. *J. Phys. Chem.* **1988**, *92*, 5674.

(24) Lifshitz, C.; Gotkis, Y.; Ioffe, A.; Laskin, J.; Shaik, S. *Int. J. Mass Spectrom. Ion Processes* **1993**, *125*, R7.

(25) Smith, B. J.; Hall, N. E. *Chem. Phys. Lett.* **1997**, *279*, 165.

(26) Ausloos, P. *J. Am. Chem. Soc.* **1982**, *104*, 5259.

(27) Buschek, J. M.; Ridal, J. J.; Holmes, J. L. *Org. Mass Spectrom* **1988**, *23*, 543.